

H. Miloudi, M. Miloudi, A. Gourbi, M.H. Bermaki, A. Bendaoud, A. Zeghoudi

A high-frequency modeling of AC motor in a frequency range from 40 Hz to 110 MHz

Introduction. Most electromagnetic compatibility models developed for the study of three-phase induction machines are generally valid for low and medium frequencies ($\ll 1$ MHz). This frequency limit seems to be too restrictive for the overall study of conducted electromagnetic interference. In this paper, the model is using the proposed model and compared with experimental results in low and medium frequency. And then, the high-frequency modeling of induction motor is presented new method based on transfer function model. The proposed methodology is verified on an experimental and simulation, it's suitable for prediction of the terminal overvoltage analysis and electromagnetic interference problems and common-mode and differential-mode currents. The **novelty** of the work consists to develop an improved high-frequency motor model based on transfer function to represent the motor high-frequency behavior for frequency-domain analyses in the frequency range from 40 Hz up to 110 MHz. The **purpose** of this work is to study the common-mode impedance and the differential-mode impedance of AC motor. The determination of these impedances is done for firstly both common and differential modes at low and medium frequency, and then common-mode and differential-mode characteristics at high frequency. **Methods.** For the study of the path of common-mode and differential-mode currents in typical AC motor (0.25 kW, 50 Hz) an identification method in high frequency for induction motor has been proposed based on the transfer function in differential-mode and common-mode configuration. The low and medium frequency model were presented in the first time based on equivalent circuit of electrical motor. Then, the common-mode and differential-mode impedances were defined in high frequency using asymptotic approach. This motor was studied by MATLAB Software for simulation and also experimental measurements. **Results.** All the simulations were performed using the mathematical model and the results obtained are validated by experimental measurements performed in the University of the Federal Armed Forces Hamburg in Germany. The obtained results of common-mode and differential-mode at low frequency, medium and high frequency are compared between simulation and experiment. References 34, table 2, figures 14.

Key words: AC motor, differential-mode, common-mode, electromagnetic interference, high frequency.

Вступ. Більшість моделей електромагнітної сумісності, розроблених для дослідження трифазних асинхронних машин, загалом застосовні для низьких та середніх частот ($\ll 1$ МГц). Ця частотна межа здається надто суворою для загального вивчення кондуктивних електромагнітних перешкод. У цій статті запропонована модель використовується і порівнюється з експериментальними результатами за низької та середньої частоти. Потім представлений новий метод високочастотного моделювання асинхронного двигуна, що базується на моделі передавальної функції. Запропонована методологія перевірена експериментально та за допомогою моделювання, вона придатна для прогнозування аналізу перенапруг на клеммах та проблем електромагнітних перешкод, а також синфазних та диференціальних струмів. **Новизна** запропонованої роботи полягає у розробці вдосконаленої моделі високочастотного двигуна на основі передавальної функції для представлення високочастотної поведінки двигуна для аналізу частотної області в діапазоні частот від 40 Гц до 110 МГц. **Мета** роботи полягає у вивченні синфазного імпедансу та диференціального імпедансу двигуна змінного струму. Визначення цих імпедансів виконується спочатку для синфазних та диференціальних мод на низькій та середній частоті, а потім для синфазних та диференціальних характеристик на високій частоті. **Методи.** Для дослідження шляху синфазних та диференціальних струмів у типовому двигуні змінного струму (0,25 кВт, 50 Гц) було запропоновано метод ідентифікації на високій частоті для асинхронного двигуна, заснований на передавальній функції у конфігураціях диференціального та синфазного режимів. Вперше представлена низько- та середньочастотна модель на основі схеми заміщення електродвигуна. Потім синфазний та диференціальний імпеданси визначені на високій частоті з використанням асимптотичного підходу. Цей двигун був вивчений програмним забезпеченням MATLAB для моделювання та експериментальних вимірювань. **Результати.** Все моделювання виконано з використанням математичної моделі, а отримані результати підтверджені експериментальними вимірами, проведеними в Університеті федеральних збройних сил у Гамбурзі, Німеччина. Отримані результати синфазного та диференціального режиму на низькій частоті, середній та високій частоті порівнюються між моделюванням та експериментом. Бібл. 34, табл. 2, рис. 14.

Ключові слова: двигун змінного струму, диференціальний режим, синфазний режим, електромагнітні завади, висока частота.

Introduction. The evaluation impedance characteristic of the induction machine in high-frequency can help study and analyze the electromagnetic interference (EMI) in adjustable drives system, so accurate modeling of induction motors in high-frequency range plays an important role in overvoltage and EMI problems [1, 2].

In association with the inverter-fed-AC motor, the motor constitutes one of the main propagation paths of common-mode (CM) and differential-mode (DM) currents [3-5]. The proposed model based on the transfer function description of the main parasitic couplings in the induction machine can be used to evaluate the high-frequency leakage currents, which are the cause of electromagnetic interference to electronic, electric equipment, and electrical networks. We developed a behavioral model allowing a better representation of impedances of the machine.

In this paper the two models are presented, the first one is shown in Fig. 1, which is valid for low and medium frequencies ($\ll 1$ MHz), this model was reported in [6-8]. After, we develop a new model for the high-frequency that is based on the asymptotical method using DM and CM impedance measurements of the induction machine.

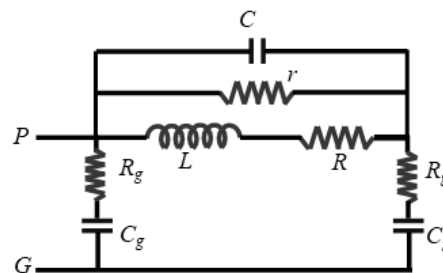


Fig. 1. Single-phase CM impedance proposed of AC motor [6, 9, 21]. Here r is stator and rotor phase resistance; L is phase leakage inductance; C is capacitance representing the turn to turn distributed capacitive coupling; R is resistance representing eddy currents inside the magnetic core and the frame; R_g is resistance representing winding-to-ground distributed resistances; C_g is capacitance representing the winding to ground distributed capacitive coupling

The proposed approach needs only the magnitude plot in the CM measurement configuration to describe the CM impedance of the AC motor, and the magnitude plot in the DM measurement configuration to describe the DM

© H. Miloudi, M. Miloudi, A. Gourbi, M.H. Bermaki, A. Bendaoud, A. Zeghoudi

impedance of the AC motor, and after we can verify the transfer function parameters of the motor by the second curve. So in this experimental setup, the motor is considered as a black box, and with frequency response, we can find the transfer function of CM and DM impedances of AC motor in a frequency range from 40 Hz up to 110 MHz.

A high-frequency induction machine model. The most frequency models of three-phase induction machines are generally constituted of a limited number of elements such as that presented in [2, 7, 9]. These models have been proposed in the literature for overvoltage and electromagnetic interference (EMI) analysis.

Many investigations into high-frequency induction motor modeling were recently reported in [6-8, 10-19]. The model presented in this work as well as those found in the literature requires the hypothesis of linearity of the machine. This assumes that the machine is never saturated. The elements depend solely on the frequency, which makes it possible to use the notion of impedance.

In [20] the influence of saturation is proved to be smaller than 2 % of the impedance's absolute value with a 5.5 kW induction machine. With frequencies higher than 80 kHz, the influence of the saturation disappears completely.

The studies in [16] have shown that the state of electromagnetic compatibility in motors, synchronous or induction, is not dependent on operating point, the high frequency (HF) model motor has the same characteristic with low speed or high speed. This enables us to restrict ourselves to identifying the machine in an off state.

The initial development of the equivalent models (Fig. 1) is generally based on an interpretation of the physical phenomena in the machine. The simplicity of this equivalent circuit gives them the advantage of being able to determine the various elements that make up them with a minimum number of measurements.

The impedance is a complex quantity, hence the magnitude and phase information are included in the impedance [22].

The magnitude Z_{DM} and phase angle $\varphi_{Z_{DM}}$ of the DM impedance of the induction machine can be evaluated respectively as:

$$Z_{DM} = \frac{K \left(\frac{1}{\omega_{n1}} \cdot s + 1 \right)}{\left[\left(\frac{1}{\omega_{n2}^2} \right) s^2 + \frac{2 \cdot \xi_2}{\omega_{n2}} s + 1 \right]}, \quad (1)$$

$$\varphi_{Z_{DM}} = \arctg \left(\frac{\omega}{\omega_1} \right) - \arctg \left(\frac{2 \cdot \xi_2 \cdot \frac{\omega}{\omega_2}}{1 - \left(\frac{\omega}{\omega_2} \right)^2} \right). \quad (2)$$

The magnitude Z_{CM} and phase angle $\varphi_{Z_{CM}}$ of the CM impedance corresponding to the circuit of Fig. 1 can be evaluated as:

$$Z_{CM} = \frac{K \cdot \left[\left(\frac{1}{\omega_{n1}^2} \right) s^2 + \frac{2 \cdot \xi_1}{\omega_{n1}} s + 1 \right]}{s \cdot \left[\left(\frac{1}{\omega_{n2}^2} \right) s^2 + \frac{2 \cdot \xi_2}{\omega_{n2}} s + 1 \right]}, \quad (3)$$

$$\varphi_{Z_{CM}} = -90 + \arctg \left(\frac{2 \cdot \xi_1 \cdot \frac{\omega}{\omega_1}}{1 - \left(\frac{\omega}{\omega_1} \right)^2} \right) - \arctg \left(\frac{2 \cdot \xi_2 \cdot \frac{\omega}{\omega_2}}{1 - \left(\frac{\omega}{\omega_2} \right)^2} \right), \quad (4)$$

where ω is the pulsation ($\omega = 2 \cdot \pi \cdot f$, where f is the frequency); s is the variable from a Laplace transform ($s = j \cdot \omega$); rest of symbols are described in Tables 1, 2.

Experimental results. The impedance Analyzer Agilent 4294A was used to measure the impedance and phase angle of the motor ranging from small size (0.25 kW – 50 Hz) in the frequency range from 40 Hz to 110 MHz.

There are two measurements conducted with the induction machine.

Differential-mode configuration. Measuring the impedance between the three-phase terminals connected and the motor neutral using the setup shown in Fig. 2 provides the DM characteristics of the induction machine under test [11, 20, 21, 23-25].

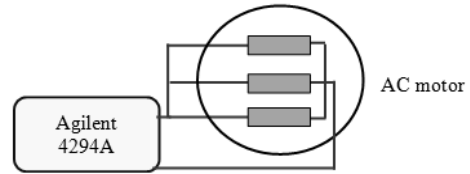


Fig. 2. DM test configuration

Fig. 3, 4 show respectively the magnitude and the phase of the measured DM characteristics as a function of frequency for 40 Hz to 110 MHz.

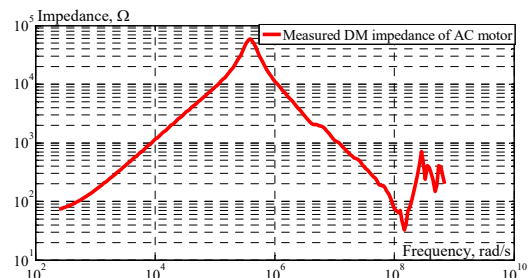


Fig. 3. DM impedance magnitude measurement

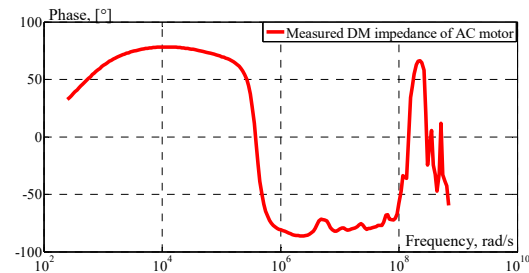


Fig. 4. DM impedance phase measurement

Common-mode configuration. Measuring three shortened phases against ground using the setup [1, 21, 23-26] shown in Fig. 5 provides the CM characteristics.

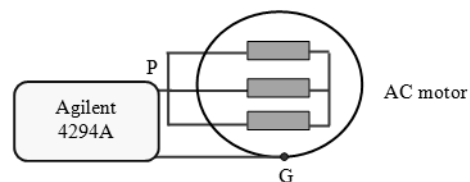


Fig. 5. CM test configuration

The evolution of the CM impedance of the motor as a function of the frequency obtained experimentally is represented in Fig. 6 (magnitude) and Fig. 7 (phase).

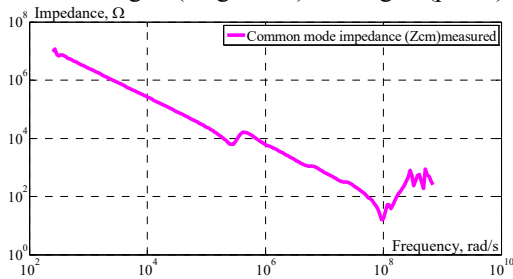


Fig. 6. CM impedance magnitude measurement

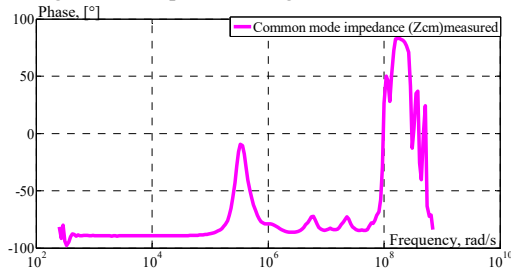


Fig. 7. CM impedance phase measurement

A high-frequency model for AC motor. In [2] and as illustrated in Fig. 3, 6, the model has been validated by DM and CM test measurements in both magnitude and phase within the frequency range from 40 Hz to 110 MHz.

The measurement impedance phase-motor neutral (Fig. 8, 9) provides the DM characteristics of the induction machine under test compared with the first proposed model shown respectively in (1) and (3).

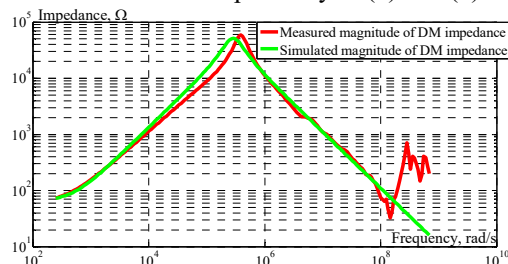


Fig. 8. Magnitude of the DM impedance

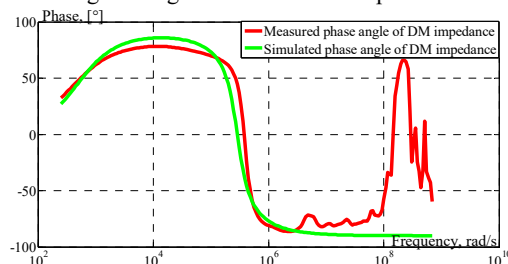


Fig. 9. Phase of the DM impedance

The values of transfer function parameters are listed in Table 1.

Constant terms K	65
The first natural frequency ω_{n1}	487
Value of zero	-487
The second natural frequency ω_{n2}	$2.88 \cdot 10^5$
Damped natural frequency ω_{b2}	$2.6713 \cdot 10^5$
Value of the first pole	$-1.07 \cdot 10^5 - j2.67 \cdot 10^5$
Value of the second pole	$-1.07 \cdot 10^5 + j2.67 \cdot 10^5$
The damping ratio ξ_2	0.371

Figures 10, 11 show the measurement CM impedance is plotted and compared with the mathematical model.

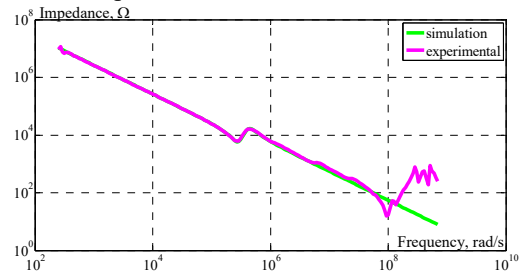


Fig. 10. Magnitude of the CM impedance

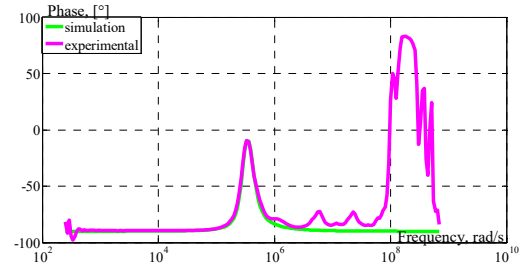


Fig. 11. Phase of the CM impedance

The values of transfer function parameters of the CM impedance are listed in Table 2.

Constant terms K	$2.62005719 \cdot 10^9$
The first natural frequency ω_{n1}	$2.87688758 \cdot 10^5$
Damped natural frequency ω_{b1}	$2.81876265 \cdot 10^5$
The second natural frequency ω_{n2}	$4.16779364 \cdot 10^5$
Damped natural frequency ω_{b2}	$4.04598107 \cdot 10^5$
The first damping ratio ξ_1	0.2
The second damping ratio ξ_2	0.24

As shown in Fig. 8–11, superimposing the experimental results and simulation results of the proposed model, we verified that there is very good accordance between them in both magnitude and phase for low and medium frequencies ($\ll 1$ MHz), and frequency components higher than 1 MHz are not able to deeply penetrate in the motor windings. For this reason, it's necessary to develop a new model in high-frequency.

A high-frequency model development for AC motor. The EMI interference levels produced by power switching converters in motor drive depend on several factors as:

- the switching frequency of the converter;
- the slope of the current and voltage at switching;
- the impedance of the main power supply;
- the length of cables from the converter to the motor.

The good evaluation of the input impedance of the system motor is key in the future evaluation of the level of the electromagnetic field around this system [27].

The most effective method in researching high-frequency characters of motor windings is multi-conductor and multi-element conducting mode [28-31] adopted lumped parameter model, this method is simplified and got the acceptable result. We proposed an approach applied to prediction the transfer function of three-phase AC motor in high-frequency, deal with the problem of building mathematical models of dynamic systems based on observed data from the motor in two configurations, CM and DM, and is thus an experimental modeling method. The proposed approach is valid for all physical models.

The system identification method base on the asymptote approach [32-34], this method is based on finding

the resonance frequencies, slopes of the asymptotes, and the terms of transfer functions corresponding to each straight line, to construct the entire transfer function of impedance in two configurations, CM and DM.

To validate the second proposed model described in this paper, two measurements were carried out on the 0.25 kW induction motor by using a Network Analyzer Agilent 4294 A in the frequency domain.

The model has been validated by DM (Fig. 12) and CM (Fig. 13) test measurements within the frequency range from 40 Hz to 110 MHz.

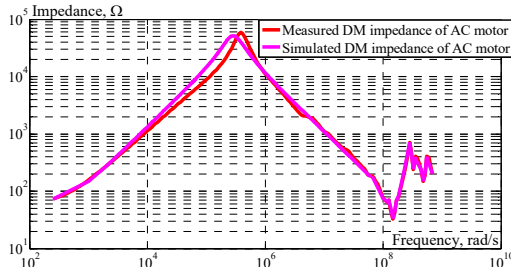


Fig. 12. Magnitude of DM impedance

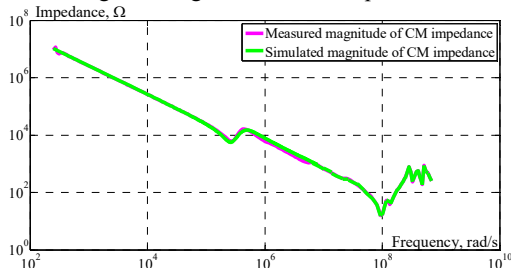


Fig. 13. Magnitude of CM impedance

The second model developed in this section is plotted with the measured results to verify that the model is an accurate representation of the machine in low, medium, and high frequencies. The plot in Fig. 12, 13 verifies that the model developed fits the measured impedance in the frequency range from 40 Hz to 110 MHz.

Analysis of HF model. HF impedances of the CM and the DM are shown in Fig. 14.

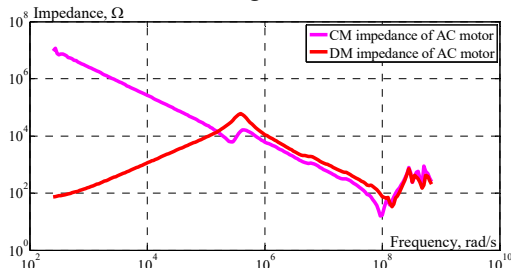


Fig. 14. Magnitude of CM impedance

The corresponding plot shown in Fig. 14 indicates that at DC the CM impedance of the induction machine behaves as an open circuit. As we increase the frequency, the impedance of the capacitor C_g dominates and decreases linearly with the frequency of slope -1 . At the first resonant frequency, the impedance of the inductor equals that of the capacitor. Above the first resonance frequency, the magnitude of the impedance of the inductor L dominates and increases of slope $+1$ until the second resonance frequency, after the impedance of the capacitor contributes and the impedance magnitude decreases with the slope of -1 . As the frequency is further increased, the CM impedance has series resonance phenomena until 110 MHz.

For the DM impedance, we can see that at low frequencies the inductor L dominates until the first resonance frequency. As the frequency increases, the capacitor C

begins to dominate at the DM resonance frequency and the impedance decreases of slope -1 . As the frequency is further increased, the DM impedance has the same series of resonance phenomena as the CM impedance.

Conclusions.

1. For the analysis of conducted EMI, it is necessary to build a satisfactory model of all parts of common-mode and differential-mode coupling paths between source and target of electromagnetic interference. Particularly for the adjustable speed drive system, the AC motor constitutes one of the main propagation paths of conducted electromagnetic perturbation.

2. In this paper, we investigated high-frequency modeling of the common-mode and differential-mode impedances of AC motors. The simulations are carried out using the proposed model in literature and compared with experimental results, making it possible to validate the first model in low and medium frequency.

3. An improved high-frequency motor model is developed to represent the motor high frequency; this model based on transfer function gives satisfactory results behavior for frequency-domain analyses in the frequency range from 40 Hz up to 110 MHz.

Acknowledgments. This research was supported by «La Direction Générale de la Recherche Scientifique et du Développement Technologique (DGRSDT)».

We would also like to show our gratitude to Stefan Dickmann, Professor, University of the Federal Armed Forces Hamburg in Germany for making measurement with us during the course of this research.

Conflict of interest. The authors declare no conflict of interest.

REFERENCES

1. Karakasli V., Ye Q., Griepentrog G., Wei J. A Parameterization of 6-Port High-Frequency Delta- and Star-Connected Induction Motor Model. *2020 International Symposium on Electromagnetic Compatibility - EMC EUROPE*, 2020, pp. 1-6. doi: <https://doi.org/10.1109/EMCEUROPE48519.2020.9245646>.
2. Wang L., Ngai-Man Ho C., Canales F., Jatskevich J. High-Frequency Modeling of the Long-Cable-Fed Induction Motor Drive System Using TLM Approach for Predicting Overvoltage Transients. *IEEE Transactions on Power Electronics*, 2010, vol. 25, no. 10, pp. 2653-2664. doi: <https://doi.org/10.1109/tpe.2010.2047027>.
3. Karimi S., Farjah E., Ghanbari T. Common and Differential Modes of Conducted Electromagnetic Interference in Electric Vehicle equipped with Supercapacitor. *2019 10th International Power Electronics, Drive Systems and Technologies Conference (PEDSTC)*, 2019. doi: <https://doi.org/10.1109/pedstc.2019.8697677>.
4. Wu Y., Yin S., Liu Z., Li H., See K.Y. Experimental Investigation on Electromagnetic Interference (EMI) in Motor Drive Using Silicon Carbide (SiC) MOSFET. *2020 International Symposium on Electromagnetic Compatibility - EMC EUROPE*, 2020, pp. 1-6. doi: <https://doi.org/10.1109/EMCEUROPE48519.2020.9245674>.
5. Guo Y., Penugonda S., Kim M., Lee J., Ha J., Yun S., Fan J., Kim H. Ground Bridge Effect on Reduction of Conducted Emission from Three-Phase Motor Drive System. *2019 International Symposium on Electromagnetic Compatibility - EMC EUROPE*, 2019, pp. 854-859. doi: <https://doi.org/10.1109/emceurope.2019.8871992>.
6. Miloudi H., Bendaoud A., Miloudi M., Dickmann S., Schenke S. Common mode and differential mode characteristics of AC motor for EMC analysis. *2016 International Symposium on Electromagnetic Compatibility - EMC EUROPE*, 2016, pp. 765-769. doi: <https://doi.org/10.1109/EMCEurope.2016.7739260>.
7. Revol B., Roudet J., Schanen J.-L., Loizelet P. EMI Study of Three-Phase Inverter-Fed Motor Drives. *IEEE Transactions on Industry Applications*, 2011, vol. 47, no. 1, pp. 223-231. doi: <https://doi.org/10.1109/TIA.2010.2091193>.
8. Degano M., Zanchetta P., Clare J., Empringham L. HF induction motor modeling using genetic algorithms and experimental impedance measurement. *2010 IEEE International Symposium on Industrial Electronics*, 2010, pp. 1296-1301. doi: <https://doi.org/10.1109/ISIE.2010.5637052>.

9. Ganjavi A., Rathnayake H., Zare F., Kumar D., Yaghoobi J., Davari P., Abbosh A. Common-Mode Current Prediction and Analysis in Motor Drive Systems for the New Frequency Range of 2–150 kHz. *IEEE Journal of Emerging and Selected Topics in Power Electronics*, 2022, vol. 10, no. 1, pp. 74-90. doi: <https://doi.org/10.1109/JESTPE.2020.3006878>.
10. Zhang Y., Li Q., Jiang D. A Motor CM Impedance Based Transformerless Active EMI Filter for DC-Side Common-Mode EMI Suppression in Motor Drive System. *IEEE Transactions on Power Electronics*, 2020, vol. 35, no. 10, pp. 10238-10248. doi: <https://doi.org/10.1109/TPEL.2020.2980881>.
11. Moreno Y., Almandoz G., Egea A., Arribas B., Urdangarin A. Analysis of Permanent Magnet Motors in High Frequency – A Review. *Applied Sciences*, 2021, vol. 11, no. 14, art. no. 6334. doi: <https://doi.org/10.3390/app11146334>.
12. Ryu Y., Han K.J. Improved transmission line model of the stator winding structure of an AC motor considering high-frequency conductor and dielectric effects. *2017 IEEE International Electric Machines and Drives Conference (IEMDC)*, 2017, pp. 1-6, doi: <https://doi.org/10.1109/IEMDC.2017.8002140>.
13. Zare F. Modeling of Electric Motors for Electromagnetic Compatibility Analysis. *Proceedings of the 2006 Australasian Universities Power Engineering Conference*, Melbourne Austria, 2006, pp. 1-5.
14. Ryu Y., Park B.-R., Han K.J. Estimation of High-Frequency Parameters of AC Machine From Transmission Line Model. *IEEE Transactions on Magnetics*, 2015, vol. 51, no. 3, pp. 1-4, art no. 8101404. doi: <https://doi.org/10.1109/TMAG.2014.2355718>.
15. Hasnaoui O. Electromagnetic interferences and common mode voltage generated by variable speed AC motors. *2014 International Conference on Electrical Sciences and Technologies in Maghreb (CISTEM)*, 2014, pp. 1-5. doi: <https://doi.org/10.1109/CISTEM.2014.7076990>.
16. Maki K., Funato H., Shao L. Motor modeling for EMC simulation by 3-D electromagnetic field analysis. *2009 IEEE International Electric Machines and Drives Conference*, 2009, pp. 103-108. doi: <https://doi.org/10.1109/IEMDC.2009.5075190>.
17. Boucenna N., Costa F., Hlioui S., Revol B. Strategy for Predictive Modeling of the Common-Mode Impedance of the Stator Coils in AC Machines. *IEEE Transactions on Industrial Electronics*, 2016, vol. 63, no. 12, pp. 7360-7371. doi: <https://doi.org/10.1109/TIE.2016.2594052>.
18. Chen H., Yan Y., Zhao H. Extraction of Common-Mode Impedance of an Inverter-Fed Induction Motor. *IEEE Transactions on Electromagnetic Compatibility*, 2016, vol. 58, no. 2, pp. 599-606. doi: <https://doi.org/10.1109/TEMC.2016.2519543>.
19. Weber S.-P., Hoene E., Guttowski S., John W., Reichl H. Modeling induction machines for EMC-Analysis. *2004 IEEE 35th Annual Power Electronics Specialists Conference*, 2004, vol. 1, pp. 94-98. doi: <https://doi.org/10.1109/PESC.2004.1355720>.
20. Boglietti A., Cavagnino A., Lazzari M. Experimental High-Frequency Parameter Identification of AC Electrical Motors. *IEEE Transactions on Industry Applications*, 2007, vol. 43, no. 1, pp. 23-29. doi: <https://doi.org/10.1109/TIA.2006.887313>.
21. Kahoul R., Marchal P., Azzouz Y., Mazari B. HF model of DC motor impedance EMC problems in automotive applications. *2008 IEEE International Symposium on Electromagnetic Compatibility*, 2008, pp. 1-5. doi: <https://doi.org/10.1109/IEMC.2008.4652143>.
22. Jia K., Bohlin G., Enohyaket M., Thottappillil R. Modelling an AC motor with high accuracy in a wide frequency range. *IET Electric Power Applications*, 2013, vol. 7, no. 2, pp. 116-122. doi: <https://doi.org/10.1049/iet-epa.2012.0127>.
23. Toulabi M.S., Wang L., Bieber L., Filizadeh S., Jatskevich J. A Universal High-Frequency Induction Machine Model and Characterization Method for Arbitrary Stator Winding Connections. *IEEE Transactions on Energy Conversion*, 2019, vol. 34, no. 3, pp. 1164-1177. doi: <https://doi.org/10.1109/TEC.2019.2891349>.
24. Hoffmann A., Ponick B. Statistical Deviation of High-Frequency Lumped Model Parameters for Stator Windings in Three-Phase Electrical Machines. *2020 International Symposium on Power Electronics, Electrical Drives, Automation and Motion (SPEEDAM)*, 2020, pp. 85-90. doi: <https://doi.org/10.1109/SPEEDAM48782.2020.9161915>.
25. Lu X., Zhang S., Liu C., Xie P., Chen H. Modeling of common-mode current in motor cable of inverter-fed motor drive system. *2016 Asia-Pacific International Symposium on Electromagnetic Compatibility (APEMC)*, 2016, pp. 511-514. doi: <https://doi.org/10.1109/APEMC.2016.7522783>.
26. Weens Y., Idir N., Franchaud J.-J., Bausiere R. Comparaison de deux méthodes de modélisation haute fréquence d'un moteur asynchrone. *Colloque International de Compatibilité Electromagnétique (CEM'06)*, Saint Malo, France, 2006, pp. 187-189. (Fra).
27. Roc'h A., Leferink F. Experimental investigation of the input common mode impedance of a motor and its cable up to 1 GHz. *2014 International Symposium on Electromagnetic Compatibility*, 2014, pp. 631-636, doi: <https://doi.org/10.1109/EMCEurope.2014.6930982>.
28. Liu J., Wang X., Jiang N. Application of ant colony algorithm to the analysis of high frequency equivalent circuit of DC motor. *WSEAS Transactions on Power Systems*, 2012, vol. 7, no. 1, pp. 1-11.
29. Liu J., Wang X., Jiang N. Study of Making Model and Simulating for DC Motor Windings Based on ACA. *2010 International Conference on Computational Intelligence and Software Engineering*, 2010, pp. 1-4. doi: <https://doi.org/10.1109/cise.2010.5676972>.
30. Benecke J., Dickmann S. Inductive and capacitive couplings in DC motors with built-in damping chokes. *2006 17th International Zurich Symposium on Electromagnetic Compatibility*, 2006, pp. 69-72. doi: <https://doi.org/10.1109/EMCZUR.2006.214871>.
31. Benecke J., Linde A., Dickmann S. Automatic HF model generation and impedance optimization for low voltage DC motors. *2008 18th International Conference on Electrical Machines*, 2008, pp. 1-6, doi: <https://doi.org/10.1109/ICELMACH.2008.4800131>.
32. Hrigua S., Costa F., Gautier C., Revol B. New modeling method based on transfer functions for EMI analysis in power electronic converters. *International Symposium on Electromagnetic Compatibility - EMC EUROPE*, 2012, pp. 1-6. doi: <https://doi.org/10.1109/EMCEurope.2012.6396839>.
33. Wu Y., Bi C., Jia K., Jin D., Li H., Yao W., Liu G. High-frequency modelling of permanent magnet synchronous motor with star connection. *IET Electric Power Applications*, 2018, vol. 12, no. 4, pp. 539-546. doi: <https://doi.org/10.1049/iet-epa.2017.0593>.
34. Miloudi H., Bendaoud A., Miloudi M., Dickmann S., Schenke S. A novel method of transfer-function identification for modeling DM impedance of AC motor. *2017 International Symposium on Electromagnetic Compatibility - EMC EUROPE*, 2017, pp. 1-5. doi: <https://doi.org/10.1109/emceurope.2017.8094770>.

Received 05.05.2022
Accepted 24.07.2022
Published 06.11.2022

Houcine Miloudi¹, Lecturer,
Mohamed Miloudi^{1,2}, Lecturer,
Abdelkader Gourbi^{3,4}, Lecturer,
Mohammed Hamza Bermaki¹, Lecturer,
Abdelber Bendaoud¹, Professor,
Abdelhakim Zeghoudi¹, PhD,

¹Laboratory of Applications of Plasma, Electrostatics and Electromagnetic Compatibility (APELEC), Djillali Liabes University Sidi-Bel-Abbes, Algeria, e-mail: el.houcine@yahoo.fr (Corresponding Author); bermaki.hamza@gmail.com; abdelber@gmail.com; hakooumzeghoudi@gmail.com

²University of Relizane, Algeria, e-mail: mohamed.miloudi@univ-relizane.dz

³Laboratory of Intelligent Control and Electrical Power Systems, Djillali Liabes University Sidi-Bel-Abbes, Algeria, e-mail: aekett@yahoo.fr

⁴Institute of Science and Applied Techniques, Ahmed Ben Bella University, Oran, Algeria

How to cite this article:

Miloudi H., Miloudi M., Gourbi A., Bermaki M.H., Bendaoud A., Zeghoudi A. A high-frequency modeling of AC motor in a frequency range from 40 Hz to 110 MHz. *Electrical Engineering & Electromechanics*, 2022, no. 6, pp. 3-7. doi: <https://doi.org/10.20998/2074-272X.2022.6.01>